*Desalination and Water Treatment*
www.deswater.com

doi:10.5004/dwt.2017.20686

72 (2017) 406–417
April

# Activated carbon derived from date stone as natural adsorbent for phenol removal from aqueous solution

Hasan Pasalari[a], Hamid Reza Ghaffari[a], Amir Hossein Mahvi[a,b,*], Mina Pourshabanian[a], Ali Azari[a]

[a]*Department of Environmental Health Engineering, School of Public Health, Tehran University of Medical Sciences, Tehran, Iran email: hasanpasalari1370@gmail.com (H. Pasalari), Ghaffarihrz@gmail.com (H.R. Ghaffari), mina.pourr@yahoo.com (M. Pourshabanian), Azari.hjh@gmail.com (A. Azari)*
[b]*Center for Solid Waste Research, Institute for Environmental Research, Tehran University of Medical Sciences, Tehran, Iran, Tel. +989123211827, Fax +982188950188, email: ahmahvi@yahoo.com (A.H. Mahvi)*

Received 19 May 2016; Accepted 6 March 2017

**ABSTRACT**

The aim of present study was to investigate the phenol adsorption onto a date stone activated carbon (DSAC) in a batch system with considering initial pH, initial phenol concentration, DSAC dosage, and contact time. Four two-parameter isotherm models (Langmuir, Freundlich, Temkin and Dubinin–Radushkevich) and four three-parameter isotherm models (Sips, Redlich-Peterson, Toth and Khan) were used to fit the experimental data. To determine the best-fit isotherm, a statistical method of Goodness of fit (GooF) was applied. An optimization method, according to standard normalized error (SNE), was used to determine the best set of parameters for each isotherm model. GooF analysis indicated that the best isotherm model to describe the phenol adsorption on surface of DSAC was Freundlich with a maximum adsorption capacity of 33.53 mg/g among the two-parameter models and Sips with a maximum adsorption capacity of 11.68 mg/g among the three-parameter isotherms. The results indicated that the DSAC is effective adsorbent for phenol removal from the aqueous solutions in terms of low cost, high availability, and easy production process.

*Keywords:* Phenol; Activated carbon; Date stone; Adsorption

## 1. Introduction

In the recent years, there has been an increasing public concern about the surface and groundwater contamination with organic compounds due to the potential for health risks related to these chemicals [1]. Phenolic compounds are the common organic contaminants in effluents of petroleum and petrochemical, coal conversion, pulp and paper, and phenol production industries [2]. The most important problems associated with these compounds are high toxicity for human and aquatic life, oxygen depletion in receiving waters, and objectionable taste and odor when react with chlorine compounds. Besides the health effects, Phenolic contamination even in low concentrations can have adverse effects on water treatment processes in terms of both efficiency and by-products production [3,4].

The solubility of phenol in water is high and the biological degradation of such compounds in water bodies is difficult. As a result, it has been frequently detected in water supplies around the world [5]. A maximum concentration level of phenol in the industrial effluents for safe discharge into surface waters is 1.0 mg/L. The World Health Organization (WHO) has assigned 0.001 mg/L as a guideline value for phenol in drinking water [6].

To date, a variety of methods have been investigated for the phenolic compounds removal from the aqueous solutions, including chemical coagulation, filtration, photo oxidation [7], sedimentation, ultra-sonication [8], Photo-sonication [9], advanced oxidation[10], and adsorption. The economical, ecological and technological advantages of adsorption

*Corresponding author.

are over remarkable than other processes [11]. Commercially activated carbon (AC) and carbon nanotubes for removing pollutants have a high production cost but, the use of agro wastes are much cheaper for applying adsorption process [12–14]. For this reason, there has been a growing attention to make the activated carbon from cheaper and renewable precursor, which exists naturally in the environment [15]. In recent years, the activated carbon obtained from various natural materials such as husk [1], laccase [16,17], peat, fly ash, bentonite [4], and kaolinite [2] have been studied for the removal of phenol from the aquatic environment.

The date may be the oldest food-producing plant known to humans in the world. Date trees are abundant in several countries such as Iran, Iraq, Saudi Arabia, Egypt, Algeria and other Mediterranean countries. The world annual production of the dates was more than 5 million tons in 2015 [10]. The date production in Iran is one million tons, annually. Date stone comprises approximately 10% of a total weight of the date. Therefore, an amount of residual date stone which can be produced annually in Iran is 100,000 tons or more. Any attempt to reuse these wastes will be useful. The most probable and applicable use for date stone is activated carbon production which can be used for contaminants removal from water and wastewater. With respect to the above, the major purposes of current study were: (1) to produce activated carbon from local date stone (Shahany) as a low-cost, abundant, and renewable precursor (2) to investigate phenol adsorption onto produced activated carbon in batch system. In addition, nonlinear regression models were used to describe adsorption data, which have approved to be more suitable than linear models in this regard. In this regard, the experimental data were fitted into four two-parameter isotherm models (Langmuir, Freundlich) and four three-parameter isotherm models (Sips, Redlich-Peterson, Toth and Khan) to determine which isotherm gives the best correlation to experimental data. Eight error functions were used to determine the best fitted isotherm which were sum of squares errors (ERRSQ/SSE), hybrid fractional error function (HYBRID), average relative error (ARE), sum of absolute error (EABS), Marquardt's percent standard deviation (MPSD), nonlinear chi-square test (X2), residual root mean square error (RMSE), average percentage errors (APE). The standard normalization error (SNE) method was used to determine the most suitable set of constants for each isotherm.

## 2. Material and methods

### 2.1. Chemicals and instruments

The chemical reagents used in this study, including-NaOH, HCl, and phenol were provided from Merck Company, Germany. Phenol in solid state was of commercial grade and used without further purification. Chemical formula and molecular weight of phenol are $C_6H_5OH$ and 94.11 (g/M), respectively. A stock solution of phenol was prepared by dissolving accurate quantities of standard powder in deionized water. The needed standard solutions were prepared from the stock solution by serial dilution. The phenol concentration was determined using UV-vis spectrophotometer (Perkin Elmer, USA) at the wavelength of 500 nm.

The date stones for activated-carbon production were provided from, Fars province, the south of Iran. Subsequent stages for active carbon production are shown in Fig. 1.

Scanning electron microscopy (SEM) analysis was carried out to study the surface morphology of prepared activated carbon. FESEM microscope (Hitachi modelS4160) at the accelerating voltage of 10 kV was used to take SEM images. The chemical functionality of DSAC and DSAC-phenol were determined with Fourier transform infrared spectroscopy (FTIR). FTIR spectra were recorded between 400 and 4000 $cm^{-1}$.

### 2.2. Batch sorption experiments

Adsorption studies were conducted in 250 ml glass Erlenmeyer flask as a reaction vessel. The experiments were performed at room temperature (about 25°C). The pH of the solution was adjusted at the desired level by adding a few drops 0.1 M NaOH or HCl solution into the flask. During the experiment, the content of the flask was agitated by a magnetic stirrer. To determine the equilibrium time of phenol adsorption onto DSAC, an accurate amount of DSAC of (0.2 g) was added to an Erlenmeyer flask containing 100 mL of phenol solution (10 mg/L). The content of flask was mixed using a magnetic stirrer. Afterward, the samples were taken at equal 15-min interval times (15, 30, 45, 60, 75, and 90 min). After the given period of time, the samples were filtered and analyzed for phenol concentration in accordance to the direct photometric method. The equilibrium time was found 60 min. In order to investigate the impact of contact time on adsorption process, 5 g DSAC was added to 100 ml phenol solution with concentration of 10 mg/L and different equal interval contact times (10, 20, 30, 40, 50, and 60).

The effect of initial phenol concentration on the phenol adsorption onto DSAC was investigated by adding 4 g/l DSAC into various flasks with different phenol concentrations (10 and 15 mg/L). After adjusting pH at 7, the content of flask was mixed using magnetic stirrer at the determined optimum time, 60 min after this period, the samples were taken and phenol concentration was determined. Each experiment was repeated three times and the average values have been reported.

To determine adsorption isotherms, different masses of DSAC (0.5, 1, 1.5, 2, 4 and 5 g) were added to 100 ml phenol solution (10 mg/L). Next, pH of the solution was adjusted at 7 and the content of flasks agitated by a magnetic stirrer at room temperature for 1.0 h. At the end of equilibrium time, the samples were taken from the flask, the liquid was filtered by 0.45 μ ceramic filter, and finally, the concentration of residual phenol was determined.

The amount phenol adsorbed onto DSAC was calculated using the following Eq. (1)[18,19].

$$q_e = \frac{(C_0 - C_e)V}{M} \quad (1)$$

Eq. (2) was used to calculate the removal the efficiency [20]:

$$\text{Removal efficiency } (\%) = \frac{100(C_0 - C_e)}{C_0} \quad (2)$$

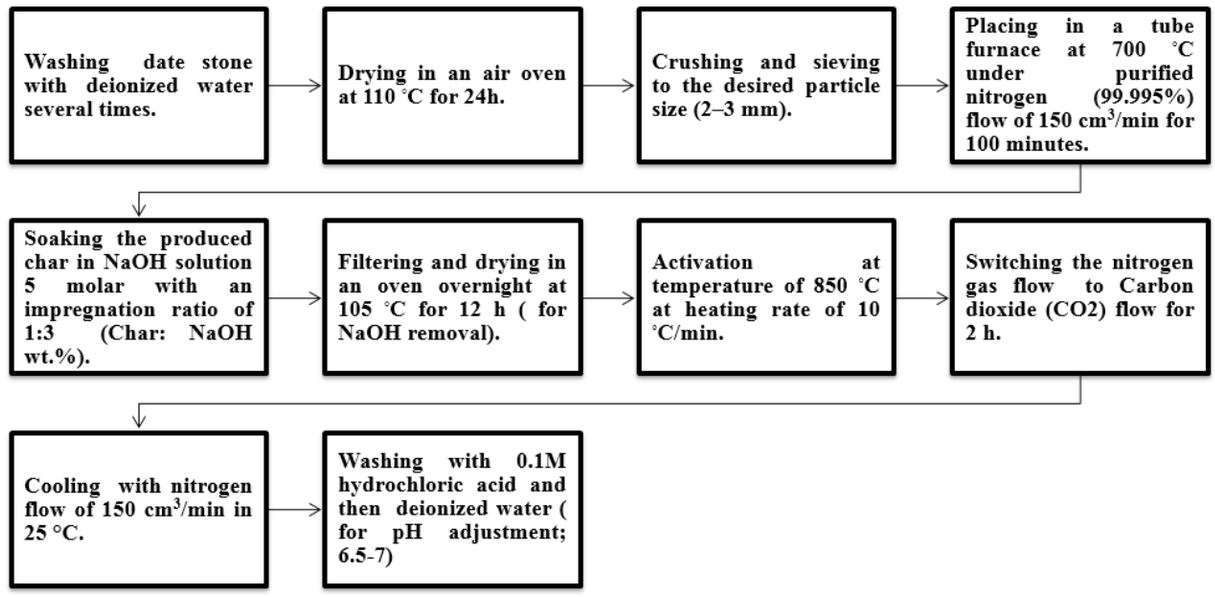


Fig. 1. Preparation stages of activated carbon.

where $C_0$ and $C_e$ (mg/L) are the liquid-phase concentrations of phenol at initial and equilibrium time, respectively. $V$ (L) is the volume of the solution and $M$ (g) is the mass of dry DSAC. Each isotherm experiment was repeated three times and the average values have been reported.

### 2.3. Isotherm models study: non-linear regression

The isotherm is mathematical equation that describes relation between amount of adsorbed adsorbate and equilibrium concentration of adsorbate in bulk solution at constant temperature [21]. In the present study, four two-parameter isotherm models (Langmuir, Freundlich, Temkin, and Dubinin-Radushkevich) and four three-parameter isotherm models (Sips, Redlich-Peterson, Toth and Khan) were fitted to the experimental data to describe the adsorption processes at the equilibrium point. These isotherm models were described in Table 1.

Non-linear regression analysis was conducted using solver Add-Ins of Microsoft Excel®, which minimize the sum of the residual error to produce the best fitness to the experimental data and to estimate the model coefficients. Optimum isotherm is selected using goodness of fit (GooF) method. In GooF method, eight error functions (Table 2) were selected and used to classify isotherms the best to the worst order. For this aim, all error functions were calculated for each isotherm and, then, the isotherm equation with the lowest error function selected as the best-fitted model to experimental data. At the first, ranking was done based on each error function and, then total ranking was conducted based on all error functions.

A different set of parameters for each isotherm might be produced by different error functions. In this study, the best ones were selected according to normalization/optimization method. In this method, the sum of normalized error (SNE) was calculated and used to select the best set

Table 1
Nonlinear form of adsorption isotherm models

| Model | Equation | Equation | Eq. | Ref. |
|---|---|---|---|---|
| Two-parameter | Langmuir | $q_e = \frac{Q_0 K_L C_e}{1 + K_L C_e}$ | 3 | [22] |
| | Freundlich | $q_e = K_F C_e^{1/n}$ | 4 | [23] |
| | Temkin | $q_e = \frac{RT}{b_T} \ln A_T C_e$ | 5 | [24] |
| | Dubinin–Radushkevich | $q_e = q_S \left[ -BRTln\left(1 + \frac{1}{C_e}\right)\right]^2$ | 6 | [25] |
| Three-parameter | Sips | $q_e = \frac{q_s K_s C_e^{m_s}}{1 + K_s C_e^{m_s}}$ | 7 | [26] |
| | Redlich–Peterson | $q_e = \frac{K_R C_e}{1 + a_R C_e^{\beta}}$ | 8 | [27] |
| | Toth | $q_e = \frac{K_T C_e}{\left(a_T + C_e\right)^{1/t}}$ | 9 | [28] |
| | Khan | $q_e = \frac{q_s b_k C_e}{\left(1 + b_k C_e\right)^{a_k}}$ | 10 | [29] |

$K_L$(L/mg), $b_T$ (KJ/mol), $K_F$ (mg/g), $B$ (mol²/kJ²), $Q_0$: maximum monolayer coverage capacities (mg/g), $n$: adsorption intensity, $A_T$: equilibrium binding constant (L/g), $q_s$: theoretical isotherm saturation capacity (mg/g), $R$: gas constant (J/mol·K), $T$: Absolute temperature (K), $C_e$: equilibrium concentration (mg/L), and $q_e$: amount of adsorbate in the adsorbent at equilibrium (mg/g).

Table 2
Different error functions and equations

| Error function | Abbreviation | Formula | Eq. | Ref. |
|---|---|---|---|---|
| Sum of squares errors | ERRSQ/SSE | $\sum_{i=1}^{n}\left(*q_{e,calc}-q_{e,\exp}\right)_i^2$ | 11 | [24] |
| Hybrid fractional error function | HYBRID | $\frac{100}{n-p}\sum_{i=1}^{n}\left(\frac{q_{e,\exp}-q_{e,calc}}{q_{e,\exp}}\right)_i$ | 12 | [30] |
| Average relative error | ARE | $\frac{100}{n}\sum_{i=1}^{n}\left\|\frac{q_{e,\exp}-q_{e,calc}}{q_{e,\exp}}\right\|$ | 13 | [31] |
| Sum of absolute error | EABS | $\sum_{i=1}^{n}\left\|q_{e,\exp}-q_{e,calc}\right\|$ | 14 | [32] |
| Marquardt's percent standard deviation | MPSD | $100\sqrt{\frac{1}{n-p}\sum_{i=1}^{n}\left(\frac{q_{e,\exp}-q_{e,calc}}{q_{e,\exp}}\right)_i^2}$ | 15 | [33] |
| Nonlinear chi-square test | $X^2$ | $\sum_{i=1}^{n}\frac{\left(q_{e,calc}-q_{e,\exp}\right)^2}{q_{e,\exp}}$ | 16 | [34] |
| Residual Root Mean Square Error | RMSE | $\sqrt{\frac{1}{n-2}\sum_{i=1}^{n}\left(q_{e,\exp}-q_{e,calc}\right)_i^2}$ | 17 | [34] |
| Average Percentage Errors | APE | $\frac{\sum_{i=}^{n}\left\|\frac{q_{e,\exp}-q_{e,calc}}{q_{e,\exp}}\right\|_i}{p}\times 100$ | 18 | [35] |

$q_{e,calc}$: Calculated amount of adsorbate in the adsorbent at equilibrium (mg/g), $q_{e,exp}$: experimental amount of adsorbate in the adsorbent at equilibrium (mg/g), $n$: Number of data point, $p$: Number of parameters within the isotherm equation.

of parameters. SNE was obtained by implementing the following steps:

1. One isotherm and one error function were selected and the isotherm parameters were determined based on trial and error method using solver Add-Ins in Microsoft Excel and the obtained parameters minimized the selected error function.
2. In this stage, the values of the other error functions for isotherm parameters set were computed,
3. The steps 1 and 2 were conducted for each isotherm and other error functions.
4. Each parameters set was selected and the ratio of its associated error functions to largest associated error function were calculated,
5. To produce sum of normalized error (SNE), obtained ratios for that parameters set were summed.
6. The parameters set with the minimum SNE was selected as the best set of parameters for that isotherm.

## 3. Result and discussion

### 3.1. Characteristics of adsorbent

#### 3.1.1. SEM image

The SEM image of raw date stone (DS), date stone activated carbon (DSAC), and DSAC after adsorption are illustrated in Fig. 2a–c. These images were taken by FESEM microscope (Hitachi modelS4160). It can be seen from Fig. 2a that the DS is formed in a concave shape with a diameter of about 25 µm and has sharp-edge shape in the range of 8 to 15 µm. However, irregular and aggregate forms of particles were observed after converting to DSAC (Fig. 2b). As can be seen from the Fig. 2c, after adsorption, significant changes occurred on the surface of DSAC due to a high rate of bonded phenol to the surface and there is a good possibility for phenol to be trapped and adsorbed into the surface of the pores.

#### 3.1.2. FTIR spectra

Fourier transform infrared (FTIR) transmission spectra were obtained to characterize the surface groups on the DSAC before and after adsorption. Fig. 3a and 3b show the FTIR spectra of the DSAC and DSAC-phenol, respectively. The most obvious peaks for DSAC are at 3400 $cm^{-1}$ which exhibit O–H groups. The peak at 1623 $cm^{-1}$ indicates stretching vibration of C=O in carboxylic acids and ketones. Broad bond at 1400 $cm^{-1}$ indicates groups containing oxygen such as C–O and C=O. C–N, and C–C functional groups and 3400 $cm^{-1}$ which show. Besides decreasing peak at 2923, for DSAC-phenol peaks were at 3400, 1623, 1033 (C–O stretching in acids), and 610 $cm^{-1}$. The most probable explanation for these changes is interaction of phenol with different functional groups on DSAC.

### 3.2. Effect of initial Phenol concentration and adsorbent dosage

The effect of initial phenol concentration on removal efficiency was examined in the concentration range of 5–20 mg/L at pH = 7, detention time of 60 min, and room temperature. As can be seen from Fig. 4, the removal efficiency increased as the initial phenol concentration increased. For example, the removal efficiency at initial concentration of 10 mg/L and DSAC dosage of 1 g/L was 52% while it was 55.5% for initial concentration of 15 mg/L at the same condition. This difference is more obvious at lower DSAC dosage and it reduces at higher DSAC dosage. The reason for higher adsorption capacity with higher initial concentration is the existence of driving force gradient originated from a higher initial concentration [36]. Another explanation for this behavior is synergistic effect due to attractive adsorbate–adsorbate interactions [37]. In addition, the removal efficiency increased from 30% to 96.7% as the DSAC dosage was increased from 0.5 to 5 g/L at detention time 60 min, and initial phenol concentration of 10 mg/L. A probable explanation for this may be more active site on surface at higher DSAC dosage. Moreover, the removal efficiency was stabilized at dosage more than 0.4 g $L^{-1}$. The most probable explanation for this is resistance to mass transfer of the phenol from bulk solution to

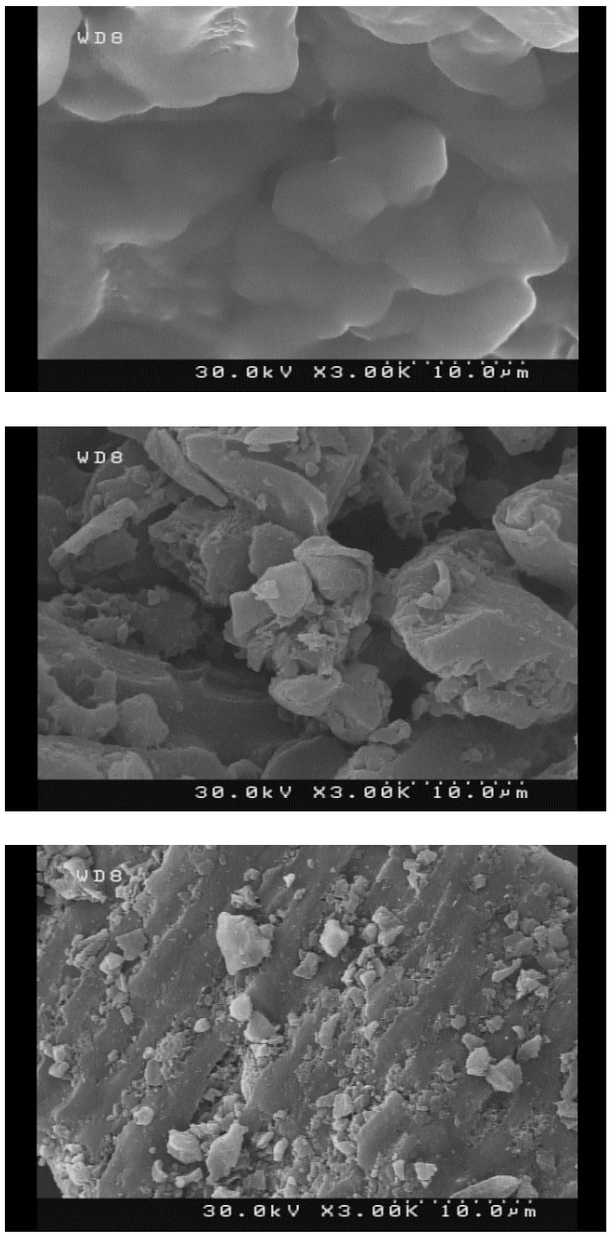


Fig. 2. SEM micrograph (magnifications: ×3.00k), a: DS; b: DSAC before adsorption; c: DSAC after adsorption.

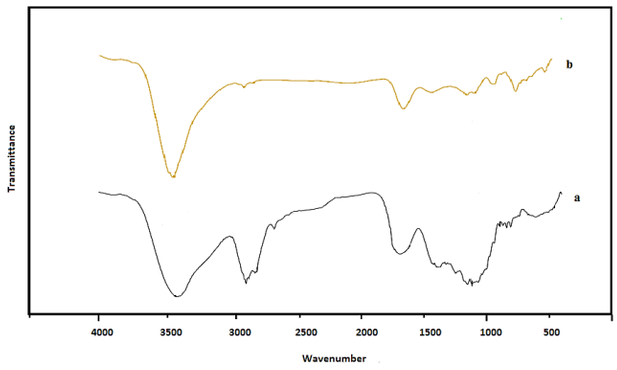


Fig. 3. FTIR spectra of DSAC and DSAC-phenol.

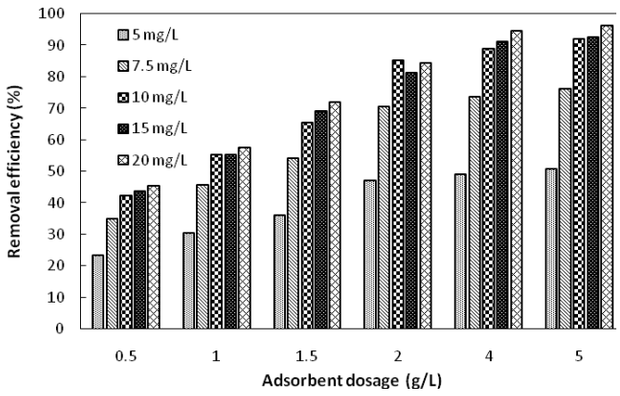


Fig. 4. The effect of adsorbent dose and phenol concentration on removal efficiency.

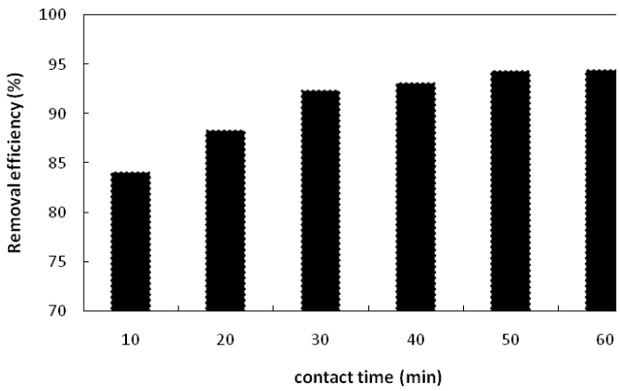


Fig. 5. The effect of contact time on the removal efficiency.

the surface of the adsorbent, which is important at high adsorbent dosage.

### 3.3. Effect of detention time on Phenol adsorption

To assess the effect of contact time on adsorption process, the experiments were conducted at contact time range 10 to 60 min with 10-min equal intervals. As can be seen from Fig. 5, increases in removal efficiency is accompanied with increases in the detention time. The process reached to the equilibrium after 60 min. Also, the adsorption was rapid at initial stages, but it became slow at higher contact time. The reasons for slow adsorption at higher contact times are that, there are less vacant sites on DSAC surface for adsorption of non-adsorbed phenol, repulsive forces between the phenol molecules on DSAC surface and the bulk solution, and less non-adsorbed molecule to be adsorbed onto adsorbent [37].

### 3.4. Adsorption isotherm

#### 3.4.1. Error analysis and model selection (GooF method)

Optimum isotherm is selected using good of fitness (GooF) method. In GooF method, eight error functions were selected (Table 2) and taken into account these error functions four two-parameter isotherms and four three-parameter isotherms were classified from the best to the worst.

The results of this analysis for two-parameter isotherms are shown in Table 3. On the basis of RMSE, ERRSQ, APE, ARE, and EABS error function, the best to the worst order for isotherms are Freundlich, Langmuir, Temkin, and Dubinin-Radushkevich. However, the results of $\chi^2$, HYBRID, and MPSD error functions are different and indicate that the best to worst order for isotherms are Dubinin-Radushkevich, Freundlich, Temkin, and Langmuir. Therefore, Freundlich isotherm was selected as the most favorable isotherm for a description of phenol adsorption on the surface of DSAC. These results are consistent to the fact that the Freundlich is the most applicable isotherm model for the description of equilibrium adsorption in water and wastewater studies (16). A possible explanation for this might be that SMCZ had heterogeneous surfaces and the adsorption of phenol on its surface was taken place as multilayers [38,39].

The results of error analysis for three-parameter isotherm are shown in Table 3. On the basis of $\chi^2$, HYBRID,MPSD, APE, RSME and ARE error function, the best to worst order for isotherms are Sips, Redlich-Peterson, Khan, and Toth. However, the results of ERRSQ and EABS error functions are different and indicate that the best to worst order for isotherms are Redlich-Peterson, Sips, Khan and Toth. Also, the most visited three-parameter isotherm is Sips model. According to combined ranking, Sips mode has the highest fit to experimental data. According to Tables 4 and 5, three-parameter models have higher $R^2$ values and consequently lower error values in comparison with two-parameter models. This can be explained by this fact that parallel to increase in the number of model constants, decrease in the fitting error is observed because a better fit can be achieved and at the same time, the generalization bias is expected to be increased because of the larger model variability [24].

#### 3.4.2. Model constants selection: SNE

Different error functions may produce a different set of parameters for each isotherm. In this study, the best set of parameters for each isotherm was selected according to normalization/optimization method. In this method, the sum of normalized error (SNE) was calculated and used for the selection of the parameters. The best set of parameters has minimum SNE.

The results of SNE for two and three-parameter isotherms were shown in Tables 4 and 5, respectively. In the tables, the best set of parameters for each isotherm was shown as highlighted. As can be seen from the Table 4, for Langmuir, Freundlich, and Temkin, the best normalized error functions for selecting an optimum set of parameters are MPSD, RMSE, and $X^2$, respectively. For Dubinin-Radushkevich, parameters can be selected based on RMSE, ERRSQ, HYBRID, and $X^2$ error functions.

As can be seen from the Table 5, the best-normalized error function to select the best set of parameters for Sips and Redlich-Peterson models is HYBRID and for Toth and Khan Models is $X^2$. Based on Tables 4 and 5, the first four set of error functions (RMSE, $\chi^2$, ERRSQ, HYBRID) have higher $R^2$ value in comparison to second four set of error functions (MPSD, ARE, EABS, APE). Therefore, first set produce more accurate models constants. This fact is important in commercial adsorbent design because more accurate isotherm constants are related to more system design [40].

Table 3
Models ranking from the best to the worst based on GooF method

| | RMSE | SSE | X2 | ERRSQ | HYBRID | MPSD | APE | ARE | EABS | Most visited |
|---|---|---|---|---|---|---|---|---|---|---|
| Two-parameter | *FR | TE | D-B | FR | D-B | D-B | FR | FR | FR | FR |
| | TE | LA | FR | TE | FR | FR | LA | LA | TE | LA |
| | LA | FR | TE | LA | TE | LA | TE | TE | LA | TE |
| | D-B | D-B | LA | D-B | LA | TE | D-R | D-B | D-B | D-R |
| Three- parameter | S | T | S | T | S | S | S | S | R-P | S |
| | T | R-P | R-P | R-P | R-P | R-P | R-P | R-P | S | R-P |
| | R-P | S | KH | KH | KH | KH | KH | KH | KH | KH |
| | KH | KH | T | S | T | T | T | T | T | T |
| Combined | S | D-B | T | D-B | D-B | S | R-P | S | S | S |
| | T | S | KH | S | S | R-P | S | R-P | T | S |
| | KH | R-P | R-P | R-P | FR | KH | KH | KH | KH | KH |
| | R-P | T | S | T | R-P | T | T | T | R-P | T |
| | FR | KH | FR | KH | T | FR | FR | FR | FR | FR |
| | TE | FR | TE | FR | KH | LA | TE | LA | TE | TE |
| | LA | TE | LA | TE | LA | TE | LA | TE | LA | LA |
| | D-B | LA | D-B | LA | TE | D-B | D-B | D-B | D-B | DB |

*FR: Freundlich, LA: Langmuir, TE: Temkin, D-B: Dubinin-Radushkevich, S: Sips, R-P: Redlich-Peterson, T: Toth, KH: Khan

Table 4
Constants of two-parameter isotherm models obtained by minimizing different error functions

| Isotherm | Parameter | RMSE | $\chi^2$ | ERRSQ | HYBRID | MPSD | ARE | EABS | APE |
|---|---|---|---|---|---|---|---|---|---|
| Langmuir | $Q_0$ | 24.51 | 22.80 | 24.51 | 22.80 | 21.37 | 20.90 | 24.54 | 20.84 |
| | | 1.53 | 2.11 | 1.53 | 2.11 | 2.66 | 2.61 | 1.64 | 2.66 |
| | $R_L$ | 0.0316 | 0.0231 | 0.0316 | 0.0231 | 0.0185 | 0.0188 | 0.0296 | 0.0185 |
| | $R^2$ | 0.888 | 0.909 | 0.888 | 0.909 | 0.928 | 0.951 | 0.876 | 0.951 |
| Freundlich | $K_F$ | 13.15 | 12.86 | 13.15 | 12.86 | 12.68 | 12.90 | 12.90 | 12.90 |
| | $n$ | 3.00 | 2.82 | 3.00 | 2.82 | 2.67 | 2.71 | 2.71 | 2.71 |
| | $R^2$ | 0.987 | 0.984 | 0.987 | 0.984 | 0.977 | 0.977 | 0.977 | 0.977 |
| Temkin | $b_T$ | 552.6 | 574.7 | 552.6 | 574.7 | 592.2 | 593.5 | 556.1 | 590.4 |
| | $A_T$ | 25.9 | 29.4 | 25.9 | 29.4 | 31.6 | 32.3 | 30.3 | 32.1 |
| | $R^2$ | 0.984 | 0.983 | 0.984 | 0.983 | 0.979 | 0.979 | 0.976 | 0.980 |
| Dubinin-Radushkevich | $B$ | 4 ($10^{-8}$) | 4 ($10^{-8}$) | 4 ($10^{-8}$) | 4 ($10^{-8}$) | 3 ($10^{-8}$) | 3 ($10^{-8}$) | 3 ($10^{-8}$) | 3 ($10^{-8}$) |
| | $q_s$ | 190 | 190 | 190 | 190 | 190 | 190 | 190 | 190 |
| | $R^2$ | 0.818 | 0.818 | 0.818 | 0.818 | 0.762 | 0.762 | 0.762 | 0.762 |
| | $E$ | 3.5 | 3.5 | 3.5 | 3.5 | 4.1 | 4.1 | 4.1 | 4.1 |

Table 5
Constants of three-parameter isotherm models obtained by minimizing different error functions

| Isotherm | Parameter | RMSE | $\chi^2$ | ERRSQ | HYBRID | MPSD | ARE | EABS | APE |
|---|---|---|---|---|---|---|---|---|---|
| Sips | $k_s$ | 3.831 | 3.828 | 3.831 | 3.828 | 3.809 | 3.878 | 3.878 | 3.878 |
| | $q_s$ | 0.647 | 0.651 | 0.647 | 0.651 | 0.638 | 0.625 | 0.625 | 0.625 |
| | $m_s$ | 0.141 | 0.143 | 0.141 | 0.143 | 0.134 | 0.132 | 0.132 | 0.132 |
| | $R^2$ | 0.998 | 0.998 | 0.998 | 0.998 | 0.998 | 0.997 | 0.997 | 0.997 |
| Redlich-Peterson | $K_R$ | 7.394 | 7.561 | 7.398 | 7.560 | 8.459 | 8.618 | 8.618 | 8.618 |
| | $a_R$ | 1.229 | 1.277 | 1.230 | 1.277 | 1.534 | 1.523 | 1.523 | 1.523 |
| | $g$ | 0.695 | 0.689 | 0.694 | 0.689 | 0.666 | 0.675 | 0.675 | 0.675 |
| | $R^2$ | 0.998 | 0.998 | 0.998 | 0.998 | 0.998 | 0.997 | 0.997 | 0.997 |
| Toth | $K_T$ | 4.794 | 4.700 | 4.795 | 4.700 | 4.412 | 4.441 | 4.441 | 4.441 |
| | $a_T$ | 0.794 | 0.742 | 0.794 | 0.742 | 0.584 | 0.535 | 0.535 | 0.535 |
| | $t$ | 1.559 | 1.577 | 1.559 | 1.577 | 1.637 | 1.629 | 1.628 | 1.628 |
| | $R^2$ | 0.998 | 0.998 | 0.998 | 0.998 | 0.998 | 0.997 | 0.997 | 0.997 |
| Khan | $q_s$ | 4.406 | 4.210 | 4.409 | 4.211 | 3.577 | 3.682 | 3.682 | 3.682 |
| | $b_K$ | 1.263 | 1.350 | 1.262 | 1.349 | 1.713 | 1.725 | 1.725 | 1.725 |
| | $a_K$ | 0.641 | 0.634 | 0.641 | 0.634 | 0.611 | 0.621 | 0.621 | 0.621 |
| | $R^2$ | 0.998 | 0.998 | 0.998 | 0.998 | 0.998 | 0.997 | 0.997 | 0.997 |

*3.4.3. Isotherm models interpretation*

From two sections above (3.4.1 and 3.4.2), the Freundlich was selected as the best model to describe the adsorption data among the two-parameter models. The next rank was attributed to Langmuir model. Among the three-parameter models, Sips generated the best fit to the experimental data according to the error analysis. This fact can be seen in Figs. 5 and 6 in which a non-linear regression isotherm models are compared. In these Figures, the best set of constants was selected for each isotherm according to SNE and then selected constants were applied to calculate the adsorption capacity of the model. These figures confirm that Freundlich, Langmuir and Sips have the best fit to the experimental data than other isotherms. Sips is a combined form of Langmuir and Freundlich models in which the heterogeneous adsorption on adsorbent surface is predicted and the limitation of the rising adsorbate concentration related to Freundlich isotherm model is avoiding [22]. Therefore, it can be concluded that Freundlich and Langmuir are the best isotherm models for describing of phenol adsorption onto DSAC. These results are in agreement with this fact that the Langmuir and Freundlich isotherms are the most commonly used isotherms for description of equilibrium adsorption in water and wastewater[18]. The adsorption isotherms are interpreted as follows:

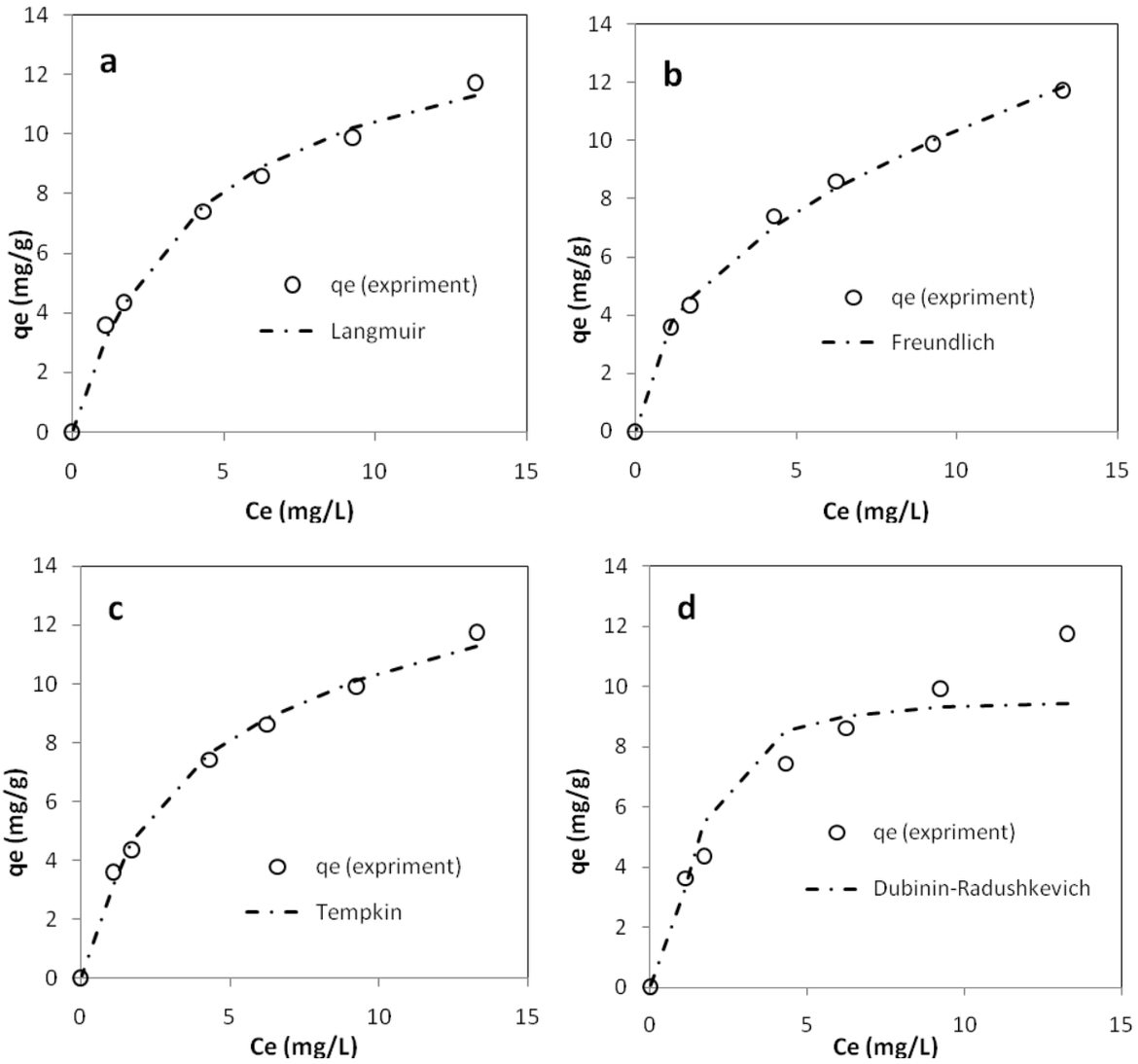


Fig. 6. Experiment and predicted two-parameter adsorption isotherm for phenol removal by DS at 60 min.

3.4.3.1. Freundlich

The Freundlich isotherm, empirical model, can be applied to non-ideal sorption on heterogeneous surfaces as multilayer sorption. The Freundlich isotherm had been derived by assuming exponentially decaying sorption energy of sites. In other word, this isotherm considers exponential distribution for active sites on the surface of the adsorbent with different adsorption energy. It is often criticized for lacking a fundamental thermodynamic basis since it does not reduce to Henry's law [41] and indefinite increase in adsorbed material as the concentration of solution is increased [42]. The Freundlich isotherm constant ($1/n$) related to adsorption intensity was found to be from 0 to 1. The values of this constant confirmed the favorability of phenol adsorption onto DSAC. The maximum adsorption capacity according to Freundlich isotherm was 13.15 mg/g.

3.4.3.2. Langmuir

The Langmuir isotherm (Eq. (4)) is logical equation in which two assumptions are considered. Firstly, there are homogenous adsorption sites on adsorbent surface [37,43] with identical binding energy [44] and same tendency to adsorbate [45]. And secondly, adsorption processes is conducted as monolayer adsorption and further adsorption cannot be taken place after that [44,46]. The essential characteristics of the Langmuir isotherm can be expressed in terms of dimensionless constant separation factor or equilibrium parameter, $R_L$ as follows:

$$R_L = \frac{1}{1 + K_L C_0} \tag{3}$$

where $b$ is Langmuir constant and $C_0$ is the highest initial concentration. At $R_L = 0$, the sorption process is irreversible,

at $R_L$ = 1 the sorption process is linear, $R_L$ > 1 at the sorption process is unfavorable, and at 0 < $R_L$ < 1 the sorption process is favorable [37]. The value of $R_L$ were found to be between 0 and 1 and confirmed that adsorption of phenol on DSAC is favorable. The maximum adsorption capacity determined by Langmuir isotherm was 24.5 mg/g.

#### 3.4.3.3. Temkin

Temkin isotherm reflects indirect interaction between adsorbate and adsorbent. For this reason, Temkin propose that adsorption heat of all molecules decrease in linear with surface coverage when extremely low and large concentration are ignored [41,47]. Adsorption energy variation ($b_T$) obtained by minimizing all error functions are positive, which indicate exothermic adsorption reaction [35]. In this study, Temkin achieved the third rank between investigated two-parameter isotherms based on error analysis. However, nonlinear data obtained by Temkin model has high agreement with experimental points ($R^2$ > 0.97).

#### 3.4.3.4. Dubinin–Radushkevich

Dubinin–Radushkevich isotherm is relatively more common than Langmuir isotherm. It is fitted successfully by process in which intermediate solute concentration is applied. It does not consider a homogenous surface or constant adsorption potential but it may be applied to predict whether the adsorption process is physical or chemical in nature with a Gaussian energy distribution onto a heterogeneous surface and through mean free energy as follows [30,48].

$$E = \frac{1}{\sqrt{2B}} \tag{4}$$

In this study, the mean $E$ value (3.5–4.1 kJ/mol) was in the range attributed to physicosorption (1–8 kJ/mol).

#### 3.4.3.5. Redlich–Peterson

Redlich–Peterson model have the advantages of both Langmuir and Freundlich equations and rectify the defects of these isotherms in some adsorption systems [49]. This model can be applied in both homogeneous and heterogeneous system. The dimensionless β value of this model can be lied between 0–1. If this value be close to unity, it means that Langmuir model can describe the adsorption data better than Freundlich model. However, in this study, the values are far from unity (0.666–0.695), which show that the isotherm follows Freundlich model better than Langmuir model, which is in agreement with error analysis results [50].

#### 3.4.3.6. Toth

The Toth isotherm is derived from potential theory and is common isotherm for description of heterogeneous adsorption process. Freundlich is not valid at low and high ends pressure range and Sips can be applied for systems with high pressure range. Toth model modifies limitations mentioned for these two models [51]. It describes a quasi-Gaussian energy distribution as well. Most available adsorption sites have energy lower than the peak or probably maximum adsorption one. $b_S$ is the Toth model constant. It is interesting to note that for $b_S$ = 1 this isotherm reduces to the Langmuir equation [52]. As can be seen from Table 5, this constant is far from unity and confirmed that adsorption process follow Freundlich better than Langmuir model as shown using error analysis results and Redlich-Peterson model constant. Ṫoth nonlinear regression curve for adsorption of phenol onto DSAC is shown in Fig. 6c. As can be seen from the figure, there is high consistency between predicted and observed adsorption capacities. This fact can be inferred from higher correlation coefficients ($R^2 \geq 0.997$) obtained by minimizing different error functions.

#### 3.4.3.7. Sips

Because of problem in Freundlich equation at high adsorbent dosage and adsorbate concentration, Sips proposed an equation which is a combination of the Langmuir and Freundlich isotherm. Sips isotherm reduces to a Freundlich isotherm at low concentrations of adsorbate, however, at high adsorbate concentrations it estimates the characteristic of a monolayer adsorption capacity of the Langmuir isotherm. In some reports, Langmuir–Freundlich (Sips) model was found most suitable for predicting the equilibrium data [53,54].

The prediction of phenol adsorption onto DSAC by the Sips model is shown in Fig. 6a.The Sips equation fits the experimental results correctly and adequately with $R^2$ value more than 0.998 for all error functions. According to Sips model, the monolayer adsorption capacity value was 94.481 mg/g (Table 5). The value of $m_s$ was far away from unity and it means that phenol adsorption data follow Freundlich form more than Langmuir model.

#### 3.4.3.8. Khan

Khan isotherm is a generalized model for the pure solutions which has proposed by Khan and Col [31]. Khan isotherm constants as well as the coefficient of determination, $R^2$, for the adsorption of phenol on to DSAC using the nonlinear regression are shown in Table 5. The values coefficients of determination, $R^2$, were as high as those of the other isotherm models. Fig. 7d shows the plots indicating experimental and predicted adsorption capacity of phenol onto DSAC by khan model. As can be seen from the figure, khan model can predict theoretical capacity with high accuracy.

## 4. Desorption study

Adsorption-desorption study of phenol by DSAC were conducted in batch reactor and its results are shown in Fig. 8. As can be seen from the figure, reduction in the ability of DSAC for reuse after 8 adsorption-desorption cycle is slight. Therefore, it can be concluded that DSAC can be used many times for phenol adsorption without much loss in initial adsorption capacity and removal efficiency. In addition, more than 70% of adsorbed phenol can be recovered in the presence of NaOH in eighth cycle, which can be used for different aims such as industrial applications.

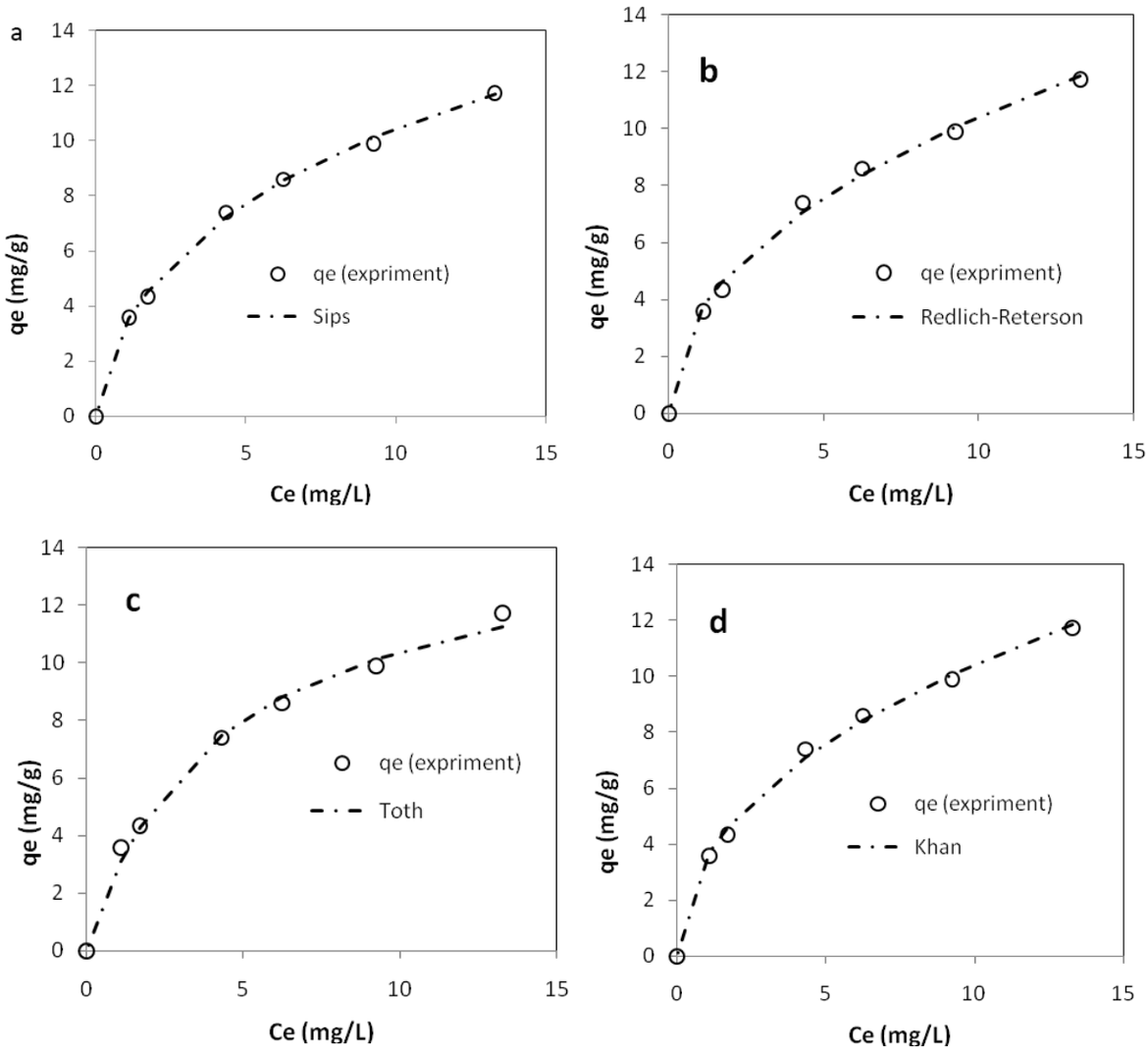


Fig. 7. Experiment and predicted three-parameter adsorption isotherm for phenol removal by DS at 60 min.

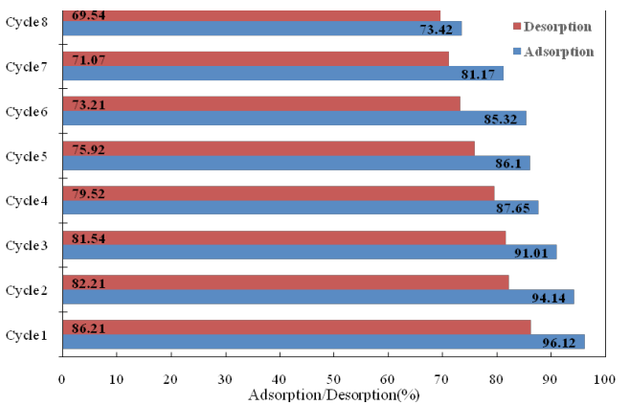


Fig. 8. Effect of desorption on the recovery on phenol from DSAC.

## 5. Probable removal mechanism

Phenol is present in water in the undissociated form. Hydrogen binding between hydroxyl group on phenol and carboxyl group on DSAC is the possible removal mechanism [55]. Electron-donor acceptor complex mechanism is another possible mechanism for phenol removal in which aromatic rings of phenol act as an electron acceptor and basic site on the surface of activated carbon act as electron donors. Furthermore, hydrophobic reactions have been suggested to be related to phenol adsorption on carbonaceous adsorbent because the adsorbate with higher hydrophobicity of phenol in aqueous solution results in stronger retaining on the carbon surface or in the pores [56]. Although phenol can be removed from aqueous solution by electrocoagulation process with good efficiency, but it is a rather expensive method and therefore our findings in this paper is more preferred as being cheaper [57].

## 6. Conclusion

In this study, the ability of activated carbon produced of date stones was investigated to remove phenol from aqueous solution. The DSAC was selected for this work because it was much cheaper and more available compared to other commercially available adsorbents. Also, the non-linear method which is more accurate than linear method was used to obtain isotherm and kinetic model fitted to adsorption data. The equilibrium data were fitted to the Langmuir, Freundlich, Temkin, and Dubinin–Radushkevich isotherms models as two-parameter isotherms as well as to the Sips, Redlich-Peterson, and Toth and-Khan Isotherms as three-parameter isotherms. Among two-parameter isotherms, the equilibrium data were best described by the Freundlich isotherm model as well as among three-parameter isotherms, the Sips was the best model to fit the experimental data. On the bases of this study, it may be concluded that date stone can be used as low-cost, natural, environmental friendly precursor to produce activated carbon for phenol removal from aqueous solutions.

## 7. Acknowledgment

The Authors would like to thank the financial grant supported by Deputy of Research, Tehran University of Medical Sciences, Tehran, Iran. Also the authors would like to acknowledge the personnel of chemistry's laboratory of Environmental Health Engineering Department, School of Public Health, Tehran University of Medical Sciences for their guidance and instrumental supports.

## References

[1] A.H. Mahvi, A. Maleki, A. Eslami, Potential of rice husk and rice husk ash for phenol removal in aqueous systems. Am. J. Appl. Sci., 1 (2004) 321–326.
[2] U.F. Alkaram, A.A. Mukhlis, A.H. Al-Dujaili, The removal of phenol from aqueous solutions by adsorption using surfactant-modified bentonite and kaolinite, J. Hazard. Mater., 169 (2009) 324–332.
[3] A.H. Mahvi, Application of agricultural fibers in pollution removal from aqueous solution, Int. J. Environ. Sci. Tech., 5 (2008) 275–285.
[4] T. Viraraghavan, F. de Maria Alfaro, Adsorption of phenol from wastewater by peat, fly ash and bentonite, J. Hazard. Mater., 57 (1998) 59–70.
[5] V.C. Srivastava, M.M. Swamy, I.D. Mall, B. Prasad, I.M. Mishra, Adsorptive removal of phenol by bagasse fly ash and activated carbon: equilibrium, kinetics and thermodynamics, Colloids Surf., A, 272 (2006) 89–104.
[6] Organization, W.H., Guidelines for drinking-water quality: recommendations. Vol. 1. (2004): World Health Organization.
[7] A.H. Mahvi, A. Maleki, M. Alimohamadi, A. Ghasri, Photo-oxidation of phenol in aqueous solution: toxicity of intermediates, Korean J. Chem. Eng., 24 (2007) 79–82.
[8] A. Maleki, A.H. ,Mahvi, A. Mesdaghinia, K. Naddafiet, Degradation and toxicity reduction of phenol by ultrasound waves, Bull. Chem. Soc. Ethiop., 21 (2007) 33–38.
[9] A.H. Mahvi, A. Maleki, Photosonochemical degradation of phenol in water, Desal. Wat. Treat., 20 (2010) 197–202.
[10] A. Maleki, A.H. Mahvi, M. Alimohamadi, A. Ghasri, Advanced oxidation of phenol by ultraviolet irradiation in aqueous system, Pak. J. Biol. Sci., 9 (2006) 38–41.
[11] J.M. Salman, V. Njoku, B.H. Hameed, Bentazon and carbofuran adsorption onto date seed activated carbon: kinetics and equilibrium, Chem. Eng. J., 173 (2011) 361–368.
[12] A.H. Mahvi, F. Gholami, S. Nazmara, Cadmium biosorption from wastewater by Ulmus leaves and their ash, Eur. J. Sci. Res., 23 (2008) 197–203.
[13] A. Maleki, A.H. Mahvi, M.A. Zazouli, H. Izanlou, A.H. Barati, Aqueous cadmium removal by adsorption on barley hull and barley hull ash, Asian J. Chem., 23 (2011) 1373–1376.
[14] M. Shirmardi, A. Mesdaghinia, A.H. Mahvi, S. Nasseri, R. Nabizadeh, Kinetics and equilibrium studies on adsorption of acid red 18 (Azo-Dye) using multiwall carbon nanotubes (MWCNTs) from aqueous solution, J. Chem., 9 (2012) 2371–2383.
[15] B.H. Hameed, J.M. Salman, A.L. Ahmad, Adsorption isotherm and kinetic modeling of 2, 4-D pesticide on activated carbon derived from date stones, J. Hazard. Mater., 163 (2009) 121–126.
[16] Z. Asadgol, H. Forootanfaret, S. Rezaei, A.H. Mahvi, Removal of phenol and bisphenol-A catalyzed by laccase in aqueous solution, JEHSE, 12 (2014) 93–98.
[17] H. Forootanfar, M.A. Faramarzi, Insights into laccase producing organisms, fermentation states, purification strategies, and biotechnological applications, Biotechnol. Progr., 31 (2015) 1443–1463.
[18] M.Y. Arıca, G. Bayramoğlu, Biosorption of Reactive Red-120 dye from aqueous solution by native and modified fungus biomass preparations of Lentinus sajor-caju, J. Hazard. Mater., 149 (2007) 499–507.
[19] M.N. Sepehr, K. Yetilmezsoy, S. Marofi, M. Zarrabi, H.R. Ghaffari, M. Fingas, M. Foroughi, Synthesis of nanosheet layered double hydroxides at lower pH: Optimization of hardness and sulfate removal from drinking water samples, JTICE, 45 (2014) 2786–2800.
[20] N.F. Cardoso, E.C. Lima, B. Royer, M.V. Bach, G.L. Dotto, L.A.A. Pinto, T. Calvete, Comparison of Spirulina platensis microalgae and commercial activated carbon as adsorbents for the removal of Reactive Red 120 dye from aqueous effluents, J. Hazard. Mater., 241–242 (2012) 146–153.
[21] N. Thinakaran, P. Panneerselvam, P. Baskaralingam, D. Elango, S. Sivanesan, Equilibrium and kinetic studies on the removal of Acid Red 114 from aqueous solutions using activated carbons prepared from seed shells, J. Hazard. Mater., 158 (2008) 142–150.
[22] A. Rahmani, M. Zarrabi, M.R. Samarghandi, A. Afkhami, H.R. Ghaffari, Degradation of Azo Dye Reactive Black 5 and acid orange 7 by Fenton-like mechanism, IAChE, 7 (2010) 87–94.
[23] R. Shokoohi, M. Saghi, H.R. Ghafari, M. Hadi, Biosorption of iron from aqueous solution by dried biomass of activated sludge, Iran. J. Environ. Health. Sci. Eng., 6 (2009) 107–114.
[24] G. McKay, A. Mesdaghinia, S. Nasseri, M. Hadi, M.S. Aminabad, Optimum isotherms of dyes sorption by activated carbon: Fractional theoretical capacity & error analysis, Chem. Eng. J., 251 (2014) 236–247.
[25] M.N. Sepehr, A. Amrane, K.A. Karimaian, M. Zarrabi, H.R. Ghaffari, Potential of waste pumice and surface modified pumice for hexavalent chromium removal: Characterization, equilibrium, thermodynamic and kinetic study, JTICE, 45 (2014) 635–647.
[26] B.H. Hameed, D.K. Mahmoud, A.L. Ahmad, Equilibrium modeling and kinetic studies on the adsorption of basic dye by a low-cost adsorbent: Coconut (Cocos nucifera) bunch waste, J. Hazard. Mater., 158 (2008) 65–72.
[27] S. Chowdhury, P. Saha, Adsorption kinetic modeling of safranin onto rice husk biomatrix using pseudo-first and pseudo-second-order kinetic models: comparison of linear and non-linear methods, CLEAN–Soil, Air, Water, 39 (2011) 274–282.
[28] S.M. Yakout, E. Elsherif, Batch kinetics, isotherm and thermodynamic studies of adsorption of strontium from aqueous solutions onto low cost rice-straw based carbons. Carbon-Sci. Technol., 1 (2010) 144–153.
[29] Y.S. Ho, G. McKay, Kinetic models for the sorption of dye from aqueous solution by wood, Process Saf. Environ. Prot., 76 (1998) 183–191.

[30] K.Y. Foo, B.H. Hameed, Insights into the modeling of adsorption isotherm systems, Chem. Eng. J., 156 (2010) 2–10.
[31] S. Shahmohammadi-Kalalagh, H.Babazadeh, Isotherms for the sorption of zinc and copper onto kaolinite: comparison of various error functions, Int. J. Environ. Sci. Technol., 11 (2014) 111–118.
[32] L.S. Chan, W.H. Cheung, S.J. Allen, G. McKay, Error analysis of adsorption isotherm models for acid dyes onto bamboo derived activated carbon, Chin. J. Chem. Eng., 20 (2012) 535–542.
[33] B. Subramanyam, A. Das, Linearized and non-linearized isotherm models comparative study on adsorption of aqueous phenol solution in soil, Int. J. Environ. Sci. Technol., 6 (2009) 633–640.
[34] M.R. Samarghandi, M. Hadi, S. Moatedi, F.A. Barjasteh, Two-parameter isotherms of methyl orange sorption by pinecone derived activated carbon, Iran. J. Environ. Health. Sci. Eng., 6 (2010) 285–294.
[35] M. Hadi, M.R. Samarghandi, G. McKay, Equilibrium two-parameter isotherms of acid dyes sorption by activated carbons: study of residual errors, Chem. Eng. J., 160 (2010) 408–416.
[36] R. Darvishi, A. Khataee, A. Koolivand, Kinetic, isotherm, and thermodynamic studies for removal of direct red 12b using nanostructured biosilica incorporated into calcium alginate matrix, Environ. Prog. Sustain Energy, 34 (2015) 1435–1443.
[37] V. Gomez, M.S. Larrechi, M.P Callao, Kinetic and adsorption study of acid dye removal using activated carbon, Chemosphere, 69 (2007) 1151–1158.
[38] D. Karadag, Y. Koc, M. Turan, M. Ozturk, A comparative study of linear and non-linear regression analysis for ammonium exchange by clinoptilolite zeolite, J. Hazard. Mater., 144 (2007) 432–437.
[39] G. Tian, W. Wang, Y. Kang, A. Wang T, Ammonium sulfide-assisted hydrothermal activation of palygorskite for enhanced adsorption of methyl violet, J. Environ. Sci., 41 (2016) 33–43.
[40] S. Rengaraj, J.W. Yeon, Y. Kim, Y. Jung, Y.K. Ha, W.H. Kim., Adsorption characteristics of Cu (II) onto ion exchange resins 252H and 1500H: kinetics, isotherms and error analysis, J. Hazard. Mater., 143 (2007) 469–477.
[41] Y.S. Ho, J.F. Porter, G McKay, Equilibrium isotherm studies for the sorption of divalent metal ions onto peat: copper, nickel and leadsingle component systems, Water, Air, Soil Pollut., 141 (2002) 1–33.
[42] (FAO), U.F.A.O., Top Ten Date Fruit Producing Countries Map. (2016).
[43] W. Konicki, D. Sibera, E. Mijowska, Z. Lendzion-Bieluń, U. Narkiewicz, Equilibrium and kinetic studies on acid dye Acid Red 88 adsorption by magnetic $ZnFe_2O_4$ spinel ferrite nanoparticles, J. Colloid Interface Sci., 398 (2013) 152–160.
[44] A. Çelekli, G. İlgün, H. Bozkurt, Sorption equilibrium, kinetic, thermodynamic, and desorption studies of Reactive Red 120 on Chara contraria, Chem. Eng. J., 191 (2012)228–235.
[45] L.M. Camacho, R.R. Parra, S. Deng, S. Deng, Arsenic removal from groundwater by MnO 2-modified natural clinoptilolite zeolite: effects of pH and initial feed concentration, J. Hazard. Mater., 189 (2011) 286–293.
[46] V.K .Jha, S. Hayashi, Modification on natural clinoptilolite zeolite for its $NH_4^+$ retention capacity, J. Hazard. Mater., 169 (2009) 29–35.
[47] X. Li, J. Wang, X. Zhang, C. ChenLi, Powdered activated carbon adsorption of two fishy odorants in water: Trans,trans-2,4-heptadienal and trans,trans-2,4-decadienal, J. Environ. Sci., 32 (2015) 15–25.
[48] A.O. Dada, A.P. Olalekan, A.M. Olatunya, O. DADA, , Langmuir, Freundlich, Temkin and Dubinin–Radushkevich isotherms studies of equilibrium sorption of $Zn^{2+}$ unto phosphoric acid modified rice husk, J. Appl. Chem., 3 (2012) 38–45.
[49] F.C. Wu, B.L. Liu, K.T. Wu, R.L. Tseng, A new linear form analysis of Redlich–Peterson isotherm equation for the adsorptions of dyes, Chem. Eng. J., 162 (2010) 21–27.
[50] Q.S. Liu, T. Zheng, P. Wang, J.P. Jiang, Adsorption isotherm, kinetic and mechanism studies of some substituted phenols on activated carbon fibers, Chem. Eng. J., 157 (2010) 348–356.
[51] A.P. Terzyk, J. Chatłas, P.A. Gauden, G. Rychlicki, Piotr Kowalczyk, Developing the solution analogue of the Toth adsorption isotherm equation, J. Colloid Interface Sci., 266 (2003) 473–476.
[52] M.M. Montazer-Rahmati, P. Rabbani, A. Abdolali, A.R. Keshtkar, Kinetics and equilibrium studies on biosorption of cadmium, lead, and nickel ions from aqueous solutions by intact and chemically modified brown algae, J. Hazard. Mater., 1 (2011) 401–407.
[53] A. Günay, E. Arslankaya, I. Tosun, Lead removal from aqueous solution by natural and pretreated clinoptilolite: adsorption equilibrium and kinetics, J. Hazard. Mater., 146 (2007) 362–371.
[54] O. Hamdaoui, E. Naffrechoux, Modeling of adsorption isotherms of phenol and chlorophenols onto granular activated carbon: Part II. Models with more than two parameters, J. Hazard. Mater., 147 (2007) 401–411.
[55] R.S. Juang, F.C. Wu, R.L. Tseng, Mechanism of adsorption of dyes and phenols from water using activated carbons prepared from plum kernels, J. Colloid Interface Sci., 227 (2000) 437–444.
[56] M.H. El-Naas, S. Al-Zuhair, M.A. Alhaija, Removal of phenol from petroleum refinery wastewater through adsorption on date-pit activated carbon, Chem. Eng. J., 162 (2010) 997–1005.